Globular Clusters as laboratories of physics beyond the standard model: Neutrino magnetic moment and Axions.

Nicolás Viaux M (PUC)

Collaborators: M. Catelan (PUC), G. Raffelt (MPP), J. Redondo (MPP), P. Stetson (DAO), A. Valcarce (PUC), A. Weiss (MPA).

Based on Viaux et al. 2013 (A&A) and Viaux et al. 2013 (PRL).

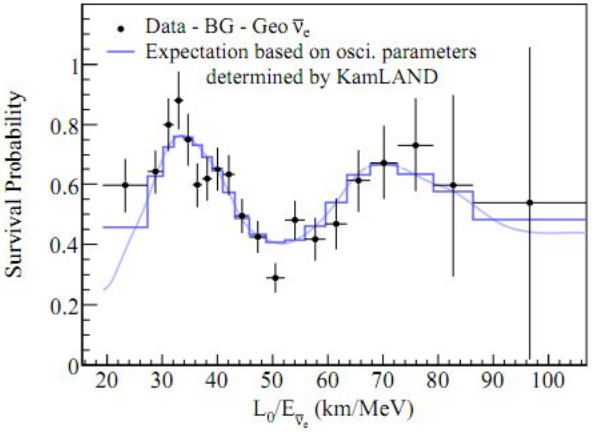

Abe et al. 2008 (KamLAND Collaboration)

Dirac neutrinos ($\nu_\alpha \neq \overline{\nu}_\alpha$)

$$\frac{\mu_\nu}{\mu_B} = \frac{6\sqrt{2} G_F m_e}{(4\pi)^2} m_\nu = 3.20 \times 10^{-19} \frac{m_\nu}{eV}$$

(Fujikawa et al. 1980), $\mu_\nu^2 = \sum_{i,j=1}^{3} \left(|\mu_{ij}|^2 + |\epsilon_{ij}|^2 \right)$.

Dirac neutrinos ($\nu_\alpha \neq \overline{\nu}_\alpha$)

$$\frac{\mu_\nu}{\mu_B} = \frac{6\sqrt{2}G_F m_e}{(4\pi)^2} m_\nu = 3.20 \times 10^{-19} \frac{m_\nu}{eV}$$

(Fujikawa et al. 1980), $\mu_\nu^2 = \sum_{i,j=1}^{3} \left(|\mu_{ij}|^2 + |\epsilon_{ij}|^2\right)$.

Majorana neutrinos ($\nu_\alpha = \overline{\nu}_\alpha$)

$\mu_{ii} = \epsilon_{ii} = 0$.

Dirac neutrinos ($\nu_\alpha \neq \overline{\nu}_\alpha$)

$$\frac{\mu_\nu}{\mu_B} = \frac{6\sqrt{2} G_F m_e}{(4\pi)^2} m_\nu = 3.20 \times 10^{-19} \frac{m_\nu}{eV}$$

(Fujikawa et al. 1980), $\mu_\nu^2 = \sum_{i,j=1}^{3} \left(|\mu_{ij}|^2 + |\epsilon_{ij}|^2 \right)$.

Majorana neutrinos ($\nu_\alpha = \overline{\nu}_\alpha$)

$\mu_{ii} = \epsilon_{ii} = 0$.

If we take into account that neutrinos have dipole moments:

If we take into account that neutrinos have dipole moments:

- The neutrino spin precess, $\nu_L \rightleftharpoons \nu_R$ in magnetic fields.

If we take into account that neutrinos have dipole moments:

- The neutrino spin precess, $\nu_L \rightleftharpoons \nu_R$ in magnetic fields.

If we take into account that neutrinos have dipole moments:

- The neutrino spin precess, $\nu_L \rightleftharpoons \nu_R$ in magnetic fields.
- μ_ν contributes to the scattering cross section $\nu_e + e \to e + \nu$. Terrestrial experiment show that $\mu_{\overline{\nu}_e} < 3.2 \times 10^{-11} \mu_B$ at 90% CL (Beda et al. 2010).

If we take into account that neutrinos have dipole moments:

- The neutrino spin precess, $\nu_L \rightleftharpoons \nu_R$ in magnetic fields.
- μ_ν contributes to the scattering cross section $\nu_e + e \to e + \nu$. Terrestrial experiment show that $\mu_{\overline{\nu}_e} < 3.2 \times 10^{-11} \mu_B$ at 90% CL (Beda et al. 2010).

If we take into account that neutrinos have dipole moments:

- The neutrino spin precess, $\nu_L \rightleftharpoons \nu_R$ in magnetic fields.
- μ_ν contributes to the scattering cross section $\nu_e + e \to e + \nu$. Terrestrial experiment show that $\mu_{\overline{\nu}_e} < 3.2 \times 10^{-11} \mu_B$ at 90% CL (Beda et al. 2010).
- Transition moments allow the radiative decay $\nu_2 \to \nu_1 + \gamma$ (between $m_2 > m_1$), the decay rate is:

$$\Gamma_{\nu_2 \to \nu_1 + \gamma} = \frac{\mu_\nu^2}{8\pi} \left(\frac{m_2^2 - m_1^2}{m_2} \right) = 5.308 s^{-1} \left(\frac{\mu_\nu}{\mu_B} \right)^2 \left(\frac{m_\nu}{eV} \right)^3$$

If we take into account that neutrinos have dipole moments:

- The neutrino spin precess, $\nu_L \rightleftharpoons \nu_R$ in magnetic fields.
- μ_ν contributes to the scattering cross section $\nu_e + e \to e + \nu$. Terrestrial experiment show that $\mu_{\overline{\nu}_e} < 3.2 \times 10^{-11} \mu_B$ at 90% CL (Beda et al. 2010).
- Transition moments allow the radiative decay $\nu_2 \to \nu_1 + \gamma$ (between $m_2 > m_1$), the decay rate is:

$$\Gamma_{\nu_2 \to \nu_1 + \gamma} = \frac{\mu_\nu^2}{8\pi} \left(\frac{m_2^2 - m_1^2}{m_2} \right) = 5.308 s^{-1} \left(\frac{\mu_\nu}{\mu_B} \right)^2 \left(\frac{m_\nu}{eV} \right)^3$$

Plasmon Decay: $\gamma_* \rightarrow \nu\overline{\nu}$

The neutrino dipole moments enhances the decay rate $\gamma_* \rightarrow \nu\overline{\nu}$ (Bernstein et al. 1963) implying a new energy loss channel in stars, when the plasmon decay becomes important.

$$\mathcal{L}_{QCD} = \sum_n \overline{q}(\gamma_u iD_\mu - m)q_n - \frac{1}{4} G^a_{\mu\nu} G^{\mu\nu}_a + \overline{\theta} \frac{g^2}{32\pi^2} G^a_{\mu\nu} \tilde{G}^{\mu\nu}_a$$

Looking the electric dipole moment of the neutron:

$$d_n \sim \frac{e\overline{\theta} m_q}{m_n^2} \quad , \tag{1}$$

$|d_n| < 2.9 \times 10^{-26} e \cdot cm$ 90% $C.L.$ Baker et al. 2006.

$$\Longrightarrow \overline{\theta} < 10^{-10}, \text{ why so small!!!}$$

Solution:

- Deal with $\overline{\theta}$ as a dynamical variable, Peccei & Quinn 1977 $\longrightarrow \mathcal{L}_a = \frac{a}{f_a} \xi \frac{g^2}{32\pi^2} G^a_{\mu\nu} \tilde{G}^{\mu\nu}_a$ (this is the most elegant solution to the CP problem).

The KSVZ model (Shifman et al. 1980)

$$\mathcal{L}_{a\gamma} = -\frac{1}{4} g_{a\gamma} F_{\mu\nu} \tilde{F}_a^{\mu\nu} = g_{a\gamma} \vec{E} \cdot \vec{B} a$$

The DFSZ model (Dine et al. 1981)

$$\mathcal{L}_{aff} = \frac{C_f}{2f_a} \overline{\Psi}_f \gamma^u \gamma_5 \Psi_f \partial_u \phi_a$$

$$C_e = \frac{\cos^2 \beta}{3}$$

$$\boxed{g_{ae} = \frac{C_e m_e}{f_a}}$$

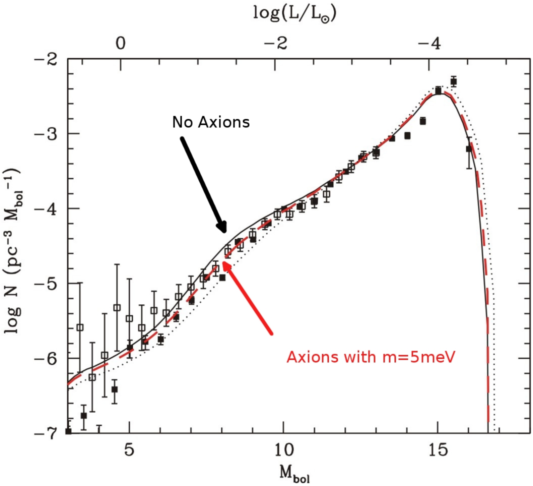

From White Dwarfs, Isern et al. 2013

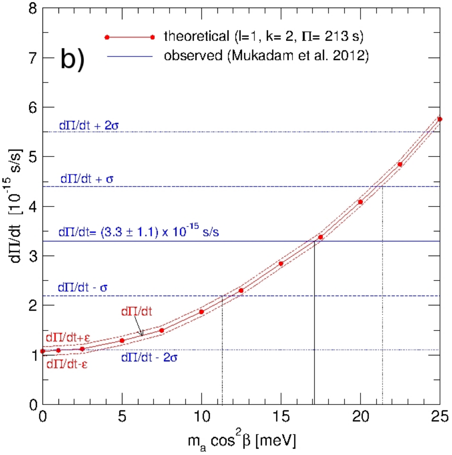

From Pulsating White Dwarfs, Córsico et al. 2012a

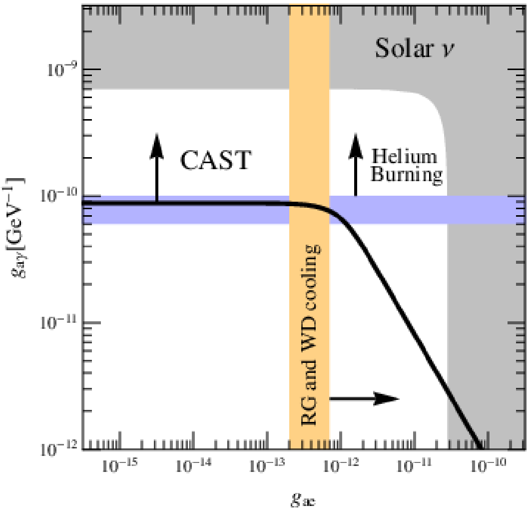

Barth et al. 2013

M3 Globular Cluster

1. ZAMS
2. Turn off
3. Helium flash
4. Horizontal Branch
5. Asymptotic Giant Branch

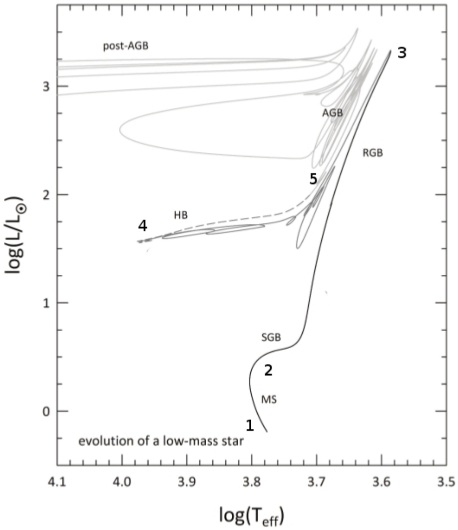

(Adapted from Catelan 2013)

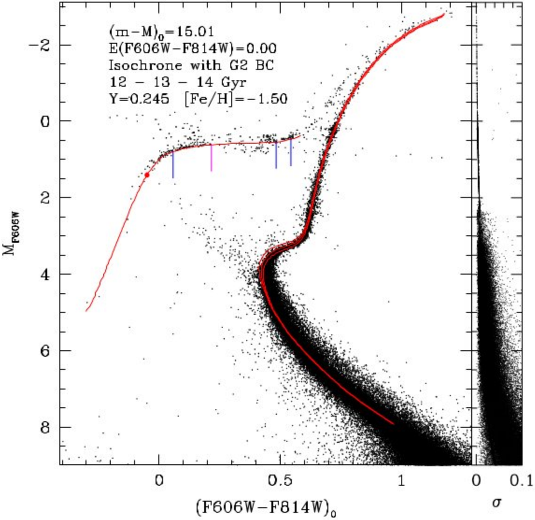

CMD of M3, A.A Valcarce PhD Thesis (2011)

Neutrino emission becomes more efficient as the star evolve. In the main sequence, neutrino emissions are due to nuclear reactions as $p + p \to d + e^+ + \nu_e$. For advanced evolutionary phases, thermal processes dominates:

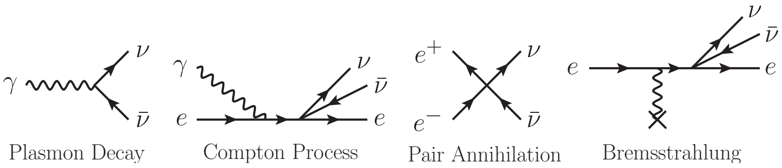

Figure : Raffelt 2012, `http://arxiv.org/abs/1201.1637`

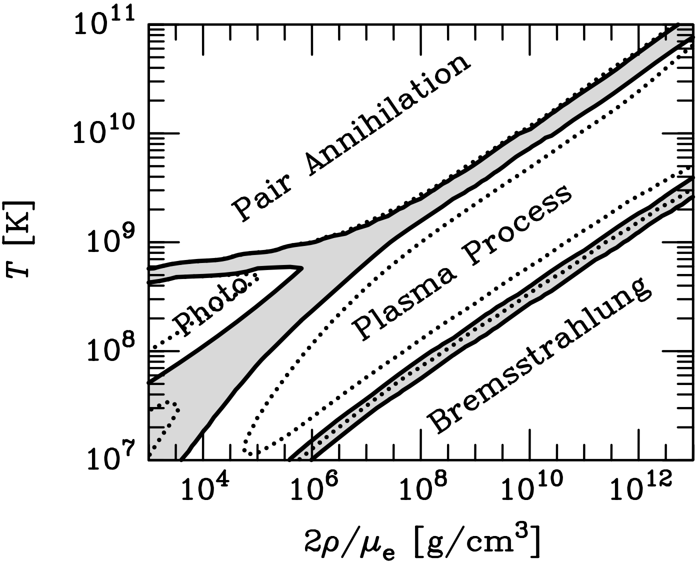

Figure : Raffelt 2012, `http://arxiv.org/abs/1201.1637`

A sensitive observable to constrain enhanced energy loss is the brightness of the tip of the red giant branch.

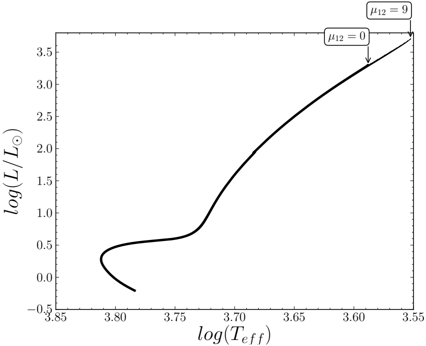

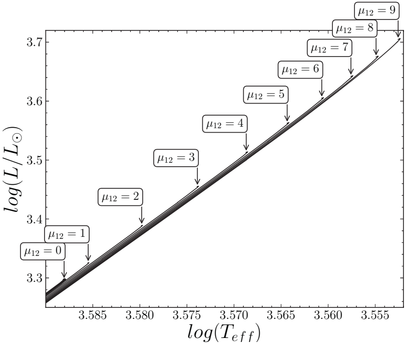

$$\mu_{12} = \mu_\nu / 10^{-12} \mu_B$$

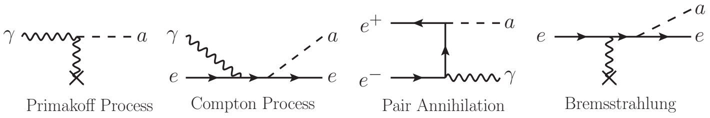

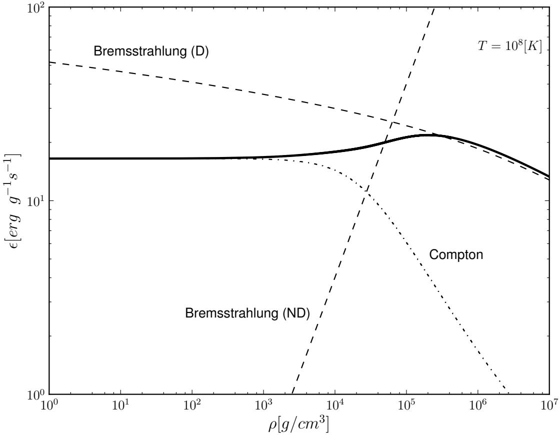

$$\epsilon_T = (\epsilon_{ND}^{-1} + \epsilon_D^{-1})^{-1} + \epsilon_C$$

(adapted from Raffelt & Weiss 1995)

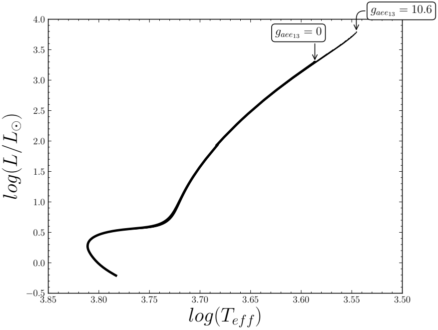

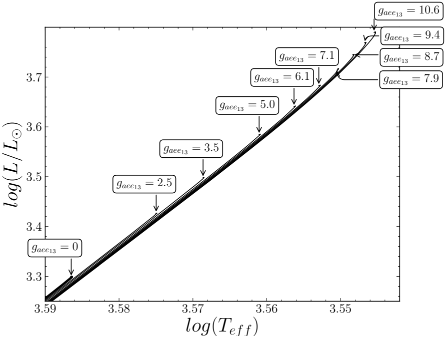

$$g_{ae_{13}} = g_{ae} \times 10^{13}$$

Globular Cluster M5 as first test.

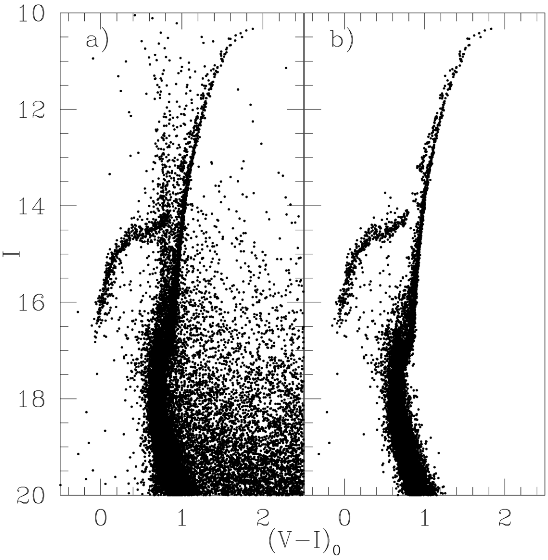

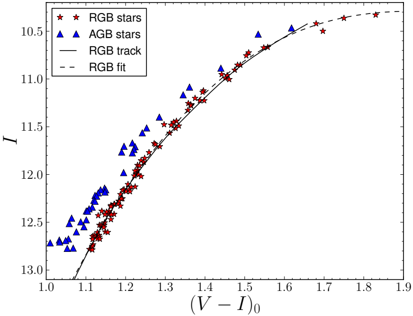

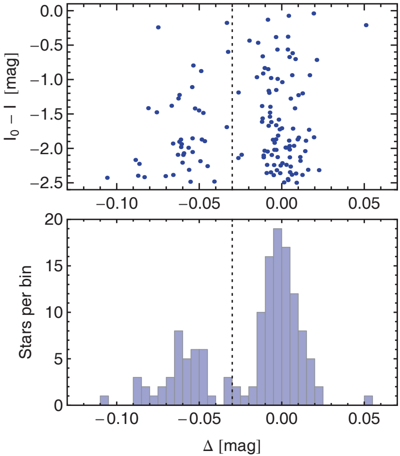

$$I = I_0 + 3.83[1.95 - (V - I)]^{2.5}$$

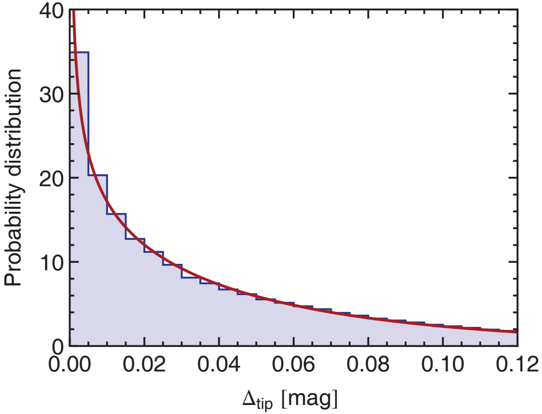

$$\langle\Delta_{\rm tip}\rangle = 0.048 \text{ mag} \quad \text{and} \quad \sigma_{\Delta_{\rm tip}} = 0.058 \text{ mag}\,,$$

Along this work, we use the Princeton-Goddard-PUC (PGPUC; Valcarce et al. 2012) stellar evolution code.

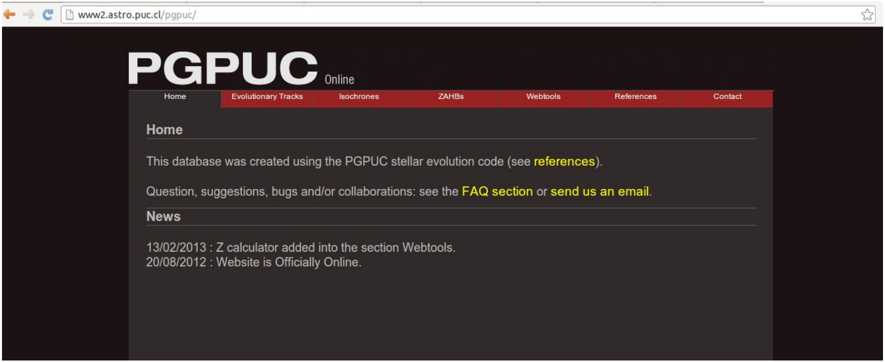

Summarizing observational uncertainties

The TRGB is located in the interval

$$M_{I,\mathrm{TRGB}}^{\mathrm{obs}} = I_1 - \langle \Delta_{\mathrm{tip}} \rangle - (m-M)_0$$

$$\Longrightarrow$$

$$M_{I,\mathrm{TRGB}}^{\mathrm{obs}} = -4.17 \pm 0.13\ \mathrm{mag}$$

This is obtained summing in quadrature the individual error sources:

- Distance modulus 0.11 mag.
- TRGB 0.058 mag.
- Calibration of the photometry, ± 0.02 mag.
- Saturation, completeness and crowding, combined contribute less than ± 0.01 mag.

Now we analyze different source of errors that can affect the TRGB in the I-band absolute magnitude. For this we use the benchmark values (for the evolutionary tracks) that is used along this work.

Mass

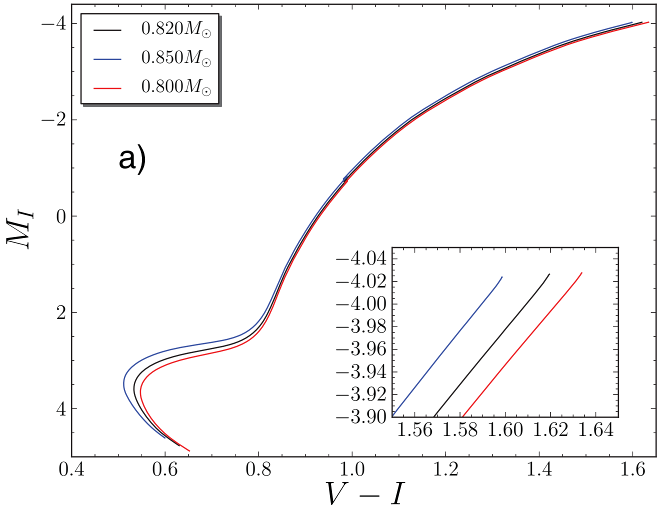
$0.820M_\odot$
$0.850M_\odot$
$0.800M_\odot$
a)
M_I
$V - I$
−4
−2
0
2
4
0.4
0.6
0.8
1.0
1.2
1.4
1.6
−4.04
−4.02
−4.00
−3.98
−3.96
−3.94
−3.92
−3.90
1.56
1.58
1.60
1.62
1.64

Helium abundance

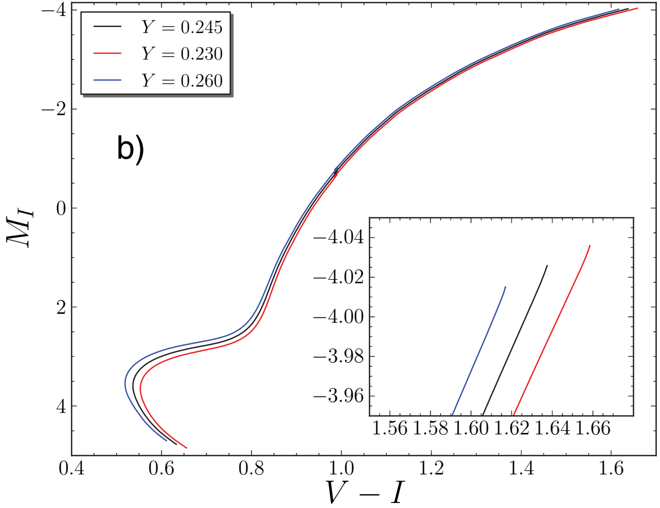

Iron abundance

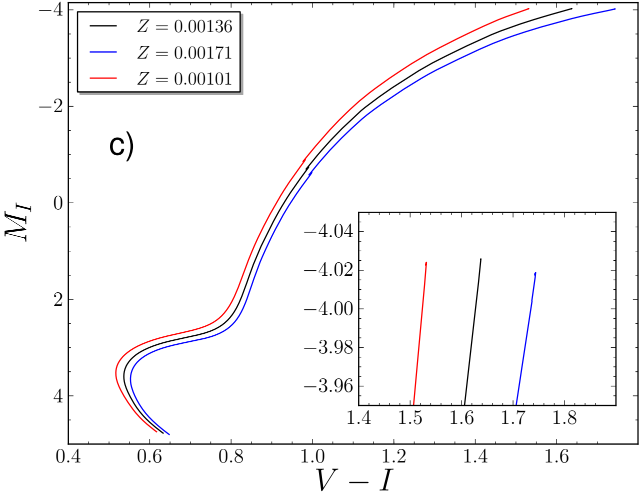

$[\alpha/Fe]$ ratio

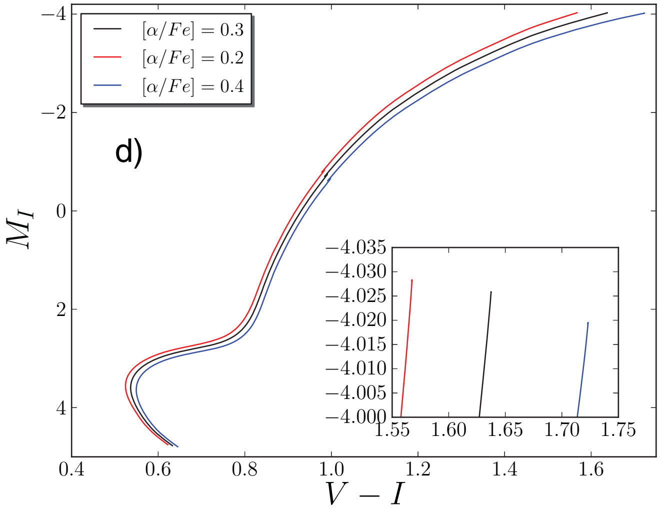

Mixing-length parameter α_{MLT}

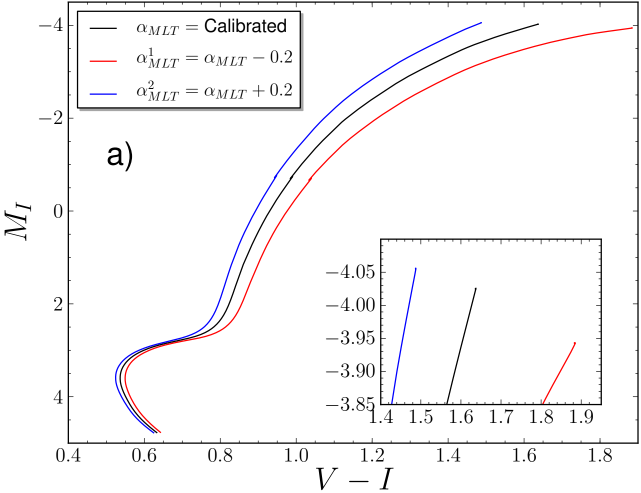

Nuclear reactions rates

Table : Changes in $M_{I,\mathrm{TRGB}}$ due to uncertainties in nuclear reaction rates

Nuclear reaction	Range	Change in $M_{I,\mathrm{TRGB}}$
$^1\mathrm{H} + {}^1\mathrm{H} \rightarrow {}^2\mathrm{H} + e^+ + \nu_e$	$\pm 3\%$	$\pm 4.06 \times 10^{-4}$ mag
$^3\mathrm{He} + {}^3\mathrm{He} \rightarrow {}^4\mathrm{He} + 2p$	$\pm 2\%$	$\pm 3.39 \times 10^{-4}$ mag
$^3\mathrm{He} + {}^4\mathrm{He} \rightarrow {}^7\mathrm{Be} + \gamma$	$\pm 6\%$	$\pm 3.70 \times 10^{-4}$ mag
$^7\mathrm{Be} + e^- \rightarrow {}^7\mathrm{Li} + \nu_e$	$\pm 10\%$	$\pm 2.27 \times 10^{-3}$ mag
$^7\mathrm{Be} + {}^1\mathrm{H} \rightarrow {}^8\mathrm{Be} + \gamma$	$\pm 3\%$	$\pm 2.03 \times 10^{-3}$ mag
$^{12}\mathrm{C} + {}^4\mathrm{He} \rightarrow {}^{16}\mathrm{O} + \gamma$	$\pm 10\%$	$\pm 1.25 \times 10^{-4}$ mag
$^4\mathrm{He} + {}^4\mathrm{He} \rightarrow {}^8\mathrm{Be} + \gamma$	$\pm 19\%$	$\pm 1.39 \times 10^{-2}$ mag
$^8\mathrm{Be} + {}^4\mathrm{He} \rightarrow {}^{12}\mathrm{C} + \gamma$	$\pm 10\%$	$\pm 7.43 \times 10^{-3}$ mag
$^{14}\mathrm{N} + p \rightarrow {}^{15}\mathrm{O} + \gamma$	$\pm 15\%$	$\mp 9.58 \times 10^{-3}$ mag
TOTAL		$\pm 1.87 \times 10^{-2}$ mag

Mass loss

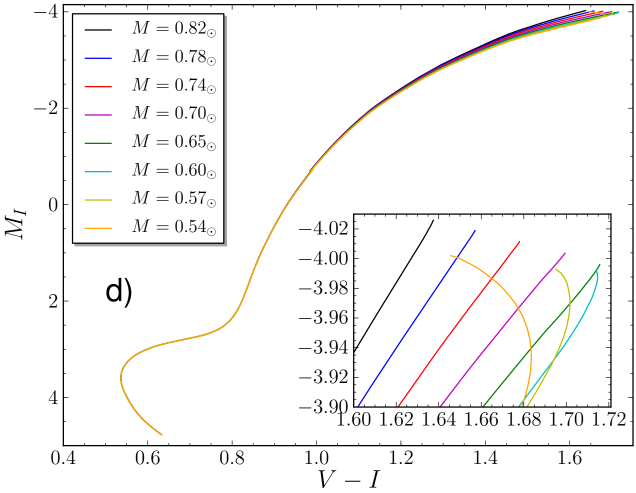
$M = 0.82_\odot$
$M = 0.78_\odot$
$M = 0.74_\odot$
$M = 0.70_\odot$
$M = 0.65_\odot$
$M = 0.60_\odot$
$M = 0.57_\odot$
$M = 0.54_\odot$
d)
M_I
$V - I$
−4
−2
0
2
4
0.4
0.6
0.8
1.0
1.2
1.4
1.6
−4.02
−4.00
−3.98
−3.96
−3.94
−3.92
−3.90
1.60
1.62
1.64
1.66
1.68
1.70
1.72

Color transformation and bolometric corrections

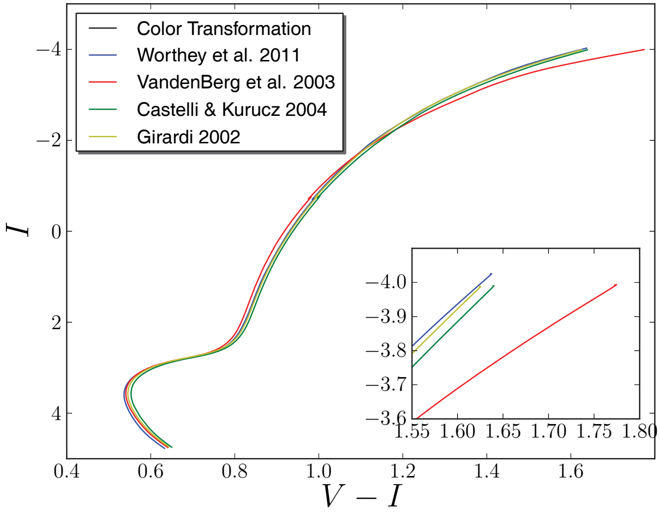

Summarizing theoretical uncertainties

Error budget in theoretically predicted $M_{I,\mathrm{TRGB}}^{\mathrm{theory}}$

Input quantity	Adopted Range	$\Delta M_{\mathrm{I,TRGB}}$ [$\times$0.01 mag]
Mass ($M_\odot$)	0.820 ± 0.025	± 0.2
Y	0.245 ± 0.015	± 1.0
Z	0.00136 ± 0.00035	$+0.7/-0$
$[\alpha/\mathrm{Fe}]$	0.3 ± 0.1	∓ 0.4
α_{MLT}	$\alpha_{\mathrm{MLT}}^{\mathrm{calibrated}} \pm 0.2$	± 5.6
Atomic diffusion	See text	$+0/-0.6$
Boundary conditions	$(1 \pm 0.05)\, T(\tau)$	∓ 0.7
κ_{rad}	$\pm 10\%$	∓ 0.02
κ_{c}	$\pm 10\%$	± 1.6
Nuclear rates	See Table 1	± 1.9
Nuclear screening	$\pm 20\%$	± 1.1

Summarizing theoretical uncertainties

Input quantity	**Adopted Range**	$\mathbf{\Delta M_{I,TRGB}}$ **[×0.01 mag]**
Neutrino emission	$\pm 5\%$	∓ 1.3
EOS	8 cases	$+2.4/-0.5$
Mass loss ($M_\odot$)	0.12–0.28	$+2.2/+3.5$

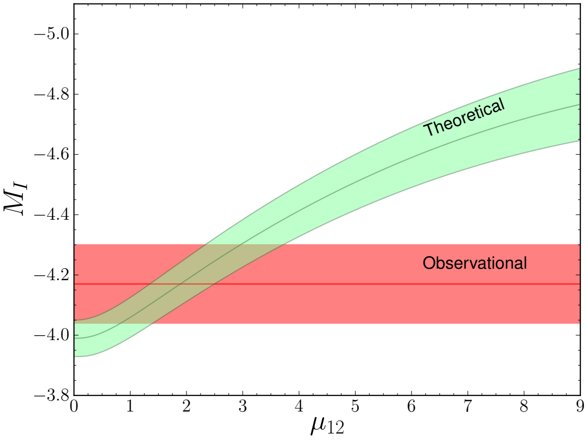
Theoretical
Observational
M_I
μ_{12}
−5.0
−4.8
−4.6
−4.4
−4.2
−4.0
−3.8
0
1
2
3
4
5
6
7
8
9

Constraints on μ_ν

$$
\begin{aligned}
\mu_\nu &< 2.6 \times 10^{-12} \quad \text{at 68\% C.L.,} \\
\mu_\nu &< 4.5 \times 10^{-12} \quad \text{at 95\% C.L.}
\end{aligned}
$$

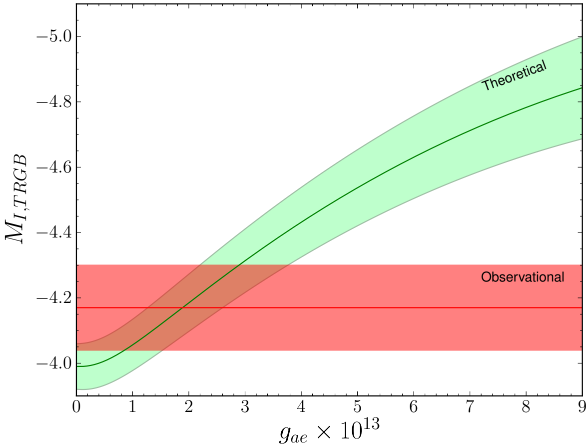
−5.0
−4.8
−4.6
−4.4
−4.2
−4.0
$M_{I,TRGB}$
Theoretical
Observational
0
1
2
3
4
5
6
7
8
9
$g_{ae} \times 10^{13}$

Constraints on g_{ae}

$$
\begin{aligned}
g_{aee} &< 2.6 \times 10^{-13} \quad \text{at } 68\% \text{ C.L.}, \\
g_{aee} &< 4.3 \times 10^{-13} \quad \text{at } 95\% \text{ C.L.}
\end{aligned}
$$

- We have used ultra-precise and homogeneous set of observations of M5.

- We have used ultra-precise and homogeneous set of observations of M5.

- We have used ultra-precise and homogeneous set of observations of M5.

- Our 1σ limits, is consistent with the constraints found in earlier works (Raffelt 1990, Raffelt & Weiss 1992, Catelan 1996), if one interpret the earlier limits at 1σ.

- We have used ultra-precise and homogeneous set of observations of M5.

- Our 1σ limits, is consistent with the constraints found in earlier works (Raffelt 1990, Raffelt & Weiss 1992, Catelan 1996), if one interpret the earlier limits at 1σ.

- Our results is more robust due that it is based on the state-of-the-art astronomical data, evolutionary calculations using up to date physical inputs.

- Our results is more robust due that it is based on the state-of-the-art astronomical data, evolutionary calculations using up to date physical inputs.

- Our results is more robust due that it is based on the state-of-the-art astronomical data, evolutionary calculations using up to date physical inputs.

- The constraints on μ_ν and g_{ae} are the most restrictive with C.L up to date.

- Our results is more robust due that it is based on the state-of-the-art astronomical data, evolutionary calculations using up to date physical inputs.

- The constraints on μ_ν and g_{ae} are the most restrictive with C.L up to date.

- Our results is more robust due that it is based on the state-of-the-art astronomical data, evolutionary calculations using up to date physical inputs.
- The constraints on μ_ν and g_{ae} are the most restrictive with C.L up to date.
- We did the same study for the Globular Cluster M3, and we obtain a very good agreement with the results showed for the M5 case.

- Our results is more robust due that it is based on the state-of-the-art astronomical data, evolutionary calculations using up to date physical inputs.
- The constraints on μ_ν and g_{ae} are the most restrictive with C.L up to date.
- We did the same study for the Globular Cluster M3, and we obtain a very good agreement with the results showed for the M5 case.